Sensors and Materials, Vol. 14, No. 6 (2002) 309–338
MYU Tokyo

S & M 0492

Production, Characteristics and Applications of Fluorescent PEBBLE Nanosensors: Potassium, Oxygen, Calcium and pH Imaging inside Live Cells

Murphy Brasuel[1], Raoul Kopelman[1*], Jonathan W. Aylott[1], Heather Clark[1], Hao Xu[1], Marion Hoyer[2], Terry J. Miller[2], Ron Tjalkens[2] and Martin A. Philbert[2]

Department of Chemistry[1] and Department of Environmental Health Sciences[2], The University of Michigan, Ann Arbor, Michigan 48109, U.S.A.

(Received October 5, 2001; accepted February 23, 2002)

Key words: optodes, PEBBLEs, nanoparticles, nanospheres, acrylamide, cross-linked decyl methacrylate, sol-gel, pH, calcium, potassium, oxygen

A novel platform for the intracellular monitoring of key biological components has been developed, using three different nanoparticle fabrication technologies. These nano-optodes are termed PEBBLEs (Probes Encapsulated By Biologically Localized Embedding). The sensors, based on polyacrylamide, cross-linked decyl methacrylate, and silica-based sol-gel, have been characterized in aqueous solution and also tested in intracellular surroundings. Each matrix can be combined with specific "free dyes", ionophores, or enzymes to produce sensors selective for the biological component of interest. Spherical sensors less than 600 nm in diameter (and reducible to below 100 nm) have been made from all three matrices. Acrylamide-based sensors have been used to monitor intracellular pH and calcium (with proven selectivity over Mg^{2+}). Decyl methacrylate has been successfully applied to intracellular potassium monitoring with probes 1,000 times more selective for potassium than sodium. Sol-gel has proven useful for monitoring intracellular oxygen at physiologically interesting concentrations. PEBBLEs, with a wide range of both simple and complex sensing schemes, provide a unique tool for minimally invasive intracellular monitoring, with many significant advantages over free dyes as well as over fiber-optic sensors.

*Corresponding author, e-mail address: kopelman@umich.edu

1. Introduction

A traditional strength of chemical sensors (optical, electrochemical, etc.) is the minimization of the *chemical interference* between the sensor and sample, achieved with the use of inert, biocompatible matrices or interfaces. However, with respect to penetrating individual live cells, the size of the sensor results in *physical interference,* accompanied by serious biological damage and resultant biochemical consequences.

Optical methods for analyzing intracellular ion concentrations have become widely used biological tools.[1–4] Injection of fluorescent indicator dyes into a cell, combined with ratiometric imaging, confocal microscopy, two-photon fluorescence, or fluorescence lifetime imaging has provided insights into concentration and spatial location of ions throughout a single cell. One challenge of using these optical methods is that each dye for use in intracellular measurements must be chosen carefully and assessed for its ability to enter and then provide accurate and reliable information from within a cell. Problems such as toxicity to the cell, intracellular sequestration, non-ratiometric properties, protein binding and intracellular buffering must be evaluated.[5–8] While some indicator dyes work well within a cell, many fluorescent probes suffer from the above problems, thus limiting the indicator dyes available for reliable intracellular measurements. For example, common calcium probes can buffer a cell when used in high concentrations,[9] and pH indicators such as carboxyfluorescein and BCECF can be affected by self-quenching and by binding to proteins.

By entrapping the indicator dyes within a polymer matrix, optodes provide a method for minimizing many of the undesired interactions that occur between fluorescent probes and the cell. The matrix allows ions or neutral analyte species to diffuse through and bind with the indicator, but prevents mobility of the indicator dyes through the cell, preventing sequestration and self-quenching. In short, the matrix protects the cell from the dyes and the dyes from cell components. Another advantage of using an optode rather than a free dye is the ability to use complex (tandem) sensing schemes to tailor selectivity, dynamic range, and the co-localization of reference dyes (to correct for light source or sensor concentration fluctuations). However, optodes have traditionally been bulky and impractical for single cell measurements, mainly due to the connecting fibers, which take up a significant amount of space inside the cell. Also, the thickness of the polymer film has prevented rapid measurements, as diffusion through the matrix can be slow. To overcome this problem, the last decade saw significant progress in miniaturization of electrodes and fiber-optic optodes.[10,11] However, even reductions to tips with 100 nm radius or below are not satisfactory.[11] In contrast, individual molecular probes (free sensing dyes) are physically sufficiently small, but usually suffer from chemical interference between the probe and cellular components. Furthermore, their use in complex, multi-dye sensing schemes is impractical.

A recent development in sensor design attempts to combine the advantages of sensor tips and molecular probes, i.e., to simultaneously avoid both physical and chemical interference between sensor (probe) and sample (cell or organelle). These spherical nanosensors have been termed PEBBLEs and, due to their chemically inert matrices and their small physical sizes, provide an almost non-perturbing, real time measurement inside intact biological systems. The small size, while important in minimizing cell perturbation,

also allows rapid measurement, because even with slow diffusion, the nanosensors reach equilibrium quickly. It also allows improved cell delivery.

The use of fluorescent indicator molecules in encapsulated form (polyacrylamide PEBBLEs) has proven valuable in the study of a number of intracellular analytes[12–15] (H^+, Ca^{2+}, Mg^{2+}, O_2). However, there are many ions for which no fluorescent indicator dye is sufficiently selective or even available. An alternate class of optical nanosensors was thus required.

Decyl methacrylate (DMA) based sensors, with much higher selectivity for most ions, relies on the chemical equilibrium (or steady state) among different sensor components. These sensors act as "bulk optodes" or ion selective optodes (ISO) where the matrix (hydrophobic liquid polymer) contains a selective lipophilic ionophore ("optically silent"), a fluoroionophore and an ionic additive.[10, 16–19] The operation of the entire system is based on having a thermodynamic equilibrium that controls ion exchange (for sensing cations) or ion co-extraction (for sensing anions), i.e., an equilibrium based correlation between different ion species. To achieve sensor miniaturization, fluorescence (rather than absorbance), has been utilized. Fabrication of PEBBLEs based on the described scheme, in the submicron size range, has been demonstrated for K^+, and extension to existing ionophores for other cations as well as anion analytes involves a simple optimization of the matrix for the required sensing elements.[20] Alternative liquid polymer sensing particles have also been recently developed by Tsagkatakis *et al.*[21] and Peper *et al.*[22] utilizing a dispersion method to cast PVC particles and plasticizer free dodecyl acrylate microspheres for ion sensing.

Sol-gel "glass" has also been used as the matrix for the fabrication of PEBBLE nanosensors, because of its superior properties over organic polymers. Sol-gel glass is a porous, high purity, optically transparent and homogeneous material,[23] thus making it an ideal choice as a sensor matrix for quantitative spectrophotometric measurements. Also, it is chemically inert, photostable and thermally stable, compared with polymer matrices. The preparation of sol-gel "glasses" is technically simple and tailoring the physicochemical properties (i.e. pore size or inner-surface hydrophobicity) of sensor materials can be achieved easily by varying the processing conditions and the amount or type of reactants used. Pore size can be optimized such that the analyte is able to diffuse easily and interact with the sensing molecules while the latter are prevented from leaking out of the matrix (also true for polyacrylamide based sensors). Furthermore, this "glass" is produced under so-called soft chemical conditions, allowing the inclusion of biomolecules.

A range of sol-gel sensor configurations has been described in the literature, including monoliths, thin films, miniaturized probe-tips and powders.[23] Immobilization of the sensing reagent in a supportive matrix is a critical step in the fabrication of optical sensors. It can be achieved by either chemical or physical entrapment (of the fluorescent dye molecules) in the pore structures of the sol-gel network. An important advantage of physical entrapment is the minimal alteration in the spectral and binding properties of the sensing molecules, due to the weak interactions with the supporting matrix. A key advantage of sol-gel sensors is that the "soft" chemical techniques used are ideal for the entrapment of enzymes and proteins. For instance, one can incorporate oxidase enzymes into proven ratiometric oxygen sensing sol-gel PEBBLEs[24] for the sensing of analytes such as glucose (using the glucose oxidase enzyme).

The nanoemulsion process for preparing PEBBLEs is subtle and there is no universal method for making hydrophilic, hydrophobic, and ampiphilic nanospheres that contain the correct matrix and chemical components, in their proper proportions. Thus, switching from single dye containing hydrophilic polyacrylamide nanospheres to multicomponent, hydrophobic, liquid polymer sensors or to inert glass sol-gel sensors is not yet a routine procedure. Specific methods for producing sensors from all these matrices are described in this report.

2. Materials and Methods

2.1 *Materials for PEBBLE production*

Reagents for PEBBLEs Acrylamide, N,N-methylenebis[acrylamide], N,N,N′,N′-tetraethylmethylenediamine (TEMED), tetraethyl orthosilicate (TEOS), hexanedioldimethacrylate (HDDMA) and kainic acid were purchased from Aldrich (Milwaukee, WI). Ammonium persulfate, Bis (2-ethylhexyl) sebacate (DOS), Brij 30, dioctyl sulfosuccinate, sodium salt (AOT), chromoionophore III or 9-(Diethylamino)-5-[(2-octoyldecyl)imino]benzo[a]phenoxazine (ETH 5350), potassium ionophore III or 2-Dodecyl-2-methyl-1,3-propanediylbis[N-[5′nitro(benzo-15-crown-5)-4′-yl]carbamate] (BME-44), potassium tetrakis-[3,5-bis(trifluoromethyl)phenyl borate (KTFPB), polyethylene glycol (PEG) 5′000 monomethyl ether, polyethylene glycol (PEG) 6′000, polyethylene glycol (PEG) 20′000, tetrahydrofuran (THF) potassium peroxodisulfate, potassium chloride (KCl), and sodium chloride (NaCl) were obtained from Fluka (Ronkonkoma, NY) and used without further purification. Decyl methacrylate (DMA) was obtained from Pfaltz & Bauer (Waterbury, CT). 5 (and 6)-carboxynaphthofluorescein (CNF), 5-(and -6-) carboxy-4′,5′-dimethylfluorescein (CDMF), 2′,7′-bis-(2-carboxypropyl)-5-(and-6)-carboxyfluorescein (BCPCF), fluorescein-5-(and -6)-sulfonic acid (FSA), 5-(and-6)-carboxy SNAFL®-1 (SNAFL), sulforhodamine 101 (SR), Calcium Crimson, Calcium Green, Calcium Orange, Calcium Green 5N and Oregon Green 488-dextran were purchased from Molecular Probes, Inc. (Eugene, OR). Ru(II)-tris(4,7-diphenyl-1,10-phenanthroline) chloride ($[Ru(dpp)_3]Cl_2$), was purchased from GFS Chemicals, Inc.(Columbus, OH). Ethanol (200 proof) was obtained from Pharmco Products Inc. (Brookfield, CT).

Gases O_2 (99.99%, extra dry grade) and N_2 (99.99%, extra dry grade) were obtained from Cryogenic Gases (Detroit, MI).

2.2 *PEBBLE fabrication*

Preparation of Polyacrylamide PEBBLEs The polymerization solution consisted of 0.4 mM fluorescent ionophore, 27% acrylamide and 3% N,N-methylenebis (acrylamide) in 0.1 M phosphate buffer, pH 6.5. One mL of this solution was then added to a solution containing 20 mL hexane, 1.8 mmol AOT and 4.24 mmol Brij 30. The solution was stirred under nitrogen for 20 min, while cooling in an ice bath. The polymerization was initiated with 24 μL of a 10% ammonium persulfate solution and 12 μL TEMED, then the solution was stirred at room temperature for 2 h. Hexane was removed by rotary evaporation, then the probes were rinsed of surfactant with ethanol, to yield a product consisting of 20 and 200 nm probes.[12,13]

Decyl methacrylate (DMA) PEBBLE Preparation A batch of PEBBLE sensors typically consisted of 210 mg of DMA, 180 mg of HDDMA, 300 mg of dioctyl sebacate, with 10–30 mmol/kg each of ionophore, chromoionophore, and ionic additives added after spherical particle synthesis. The spherical particles were prepared by dissolving decyl methacrylate, HDDMA, and DOS in 2 mL of hexane. To a 100 mL round bottom flask, in a water bath on a hot plate stirrer, 75 mL of pH 2 HCl was added along with 1.8 g of PEG 5′000 monomethyl ether, or PEG 6′000, or PEG 20′000 and stirred and degassed. The hexane dissolved monomer cocktail was then added to the reaction flask under nitrogen and stirred at full speed, and the water bath temperature was raised to 80°C over 30–40 min. 6 mg of potassium peroxodisulfate was then added to the reaction and stirring was reduced to medium speed. The temperature was kept at 80°C for two more hours, and then the reaction was allowed to return to room temperature and stirred for 8–12 h. The resulting polymer was suction filtered through a Fisherbrand glass microanalysis vacuum filter holder with a Whatman anodisc filter (0.2 μm pore diameter). The polymer was rinsed three times with water and three times with ethanol to remove excess PEG and unreacted polymer. THF was then used to leach out the DOS and then the PEBBLEs were again filtered and rinsed. They were allowed to dry in a 70°C oven overnight. Dry polymer was then weighed out, and DOS, BME-44, ETH 5350 and KTFPB were added to this dry polymer, so that the resulting polymer would have 40% DOS, 20 mmole/kg BME-44, 10 mmole/kg ETH 5350, and 10 mmole/kg KTFPB. Sufficient THF was added to this mixture to just wet the PEBBLEs. The PEBBLEs were allowed to swell for eight hours and then the THF was removed by roto-evaporation. The resulting PEBBLE sensors were rinsed with double distilled water and allowed to air dry.[20]

Preparation of Sol-Gel PEBBLEs The reaction solution consisted of PEG MW 5′000 monomethyl ether (3 g), ethanol (6 mL), Oregon Green-dextran MW 10,000 (0.1 mM), $[Ru(dpp)_3]^{2+}$ (0.4 mM), and 30% wt. ammonia water (3.9 mL) with ammonia serving as a catalyst and water being one of the reactants. Upon mixing, the solution became transparent and tetraethyl orthosilicate (TEOS) (0.5 mL) was added dropwise to initiate the hydrolysis of TEOS. The solution was then stirred at room temperature for 1 hour to allow the sol-gel reaction to reach completion.

A liberal amount of ethanol was then added to the reaction solution and the mixture was transferred to an Amicon ultrafiltration cell (Millipore Corp., Bedford, MA). A 100 kDa membrane was used to separate the reacted sol-gel particles (PEBBLEs) from the unreacted monomers, PEG, ammonia and dye molecules, under a pressure of 10 psi. The PEBBLEs were further rinsed with 500 mL ethanol to ensure that all unreacted chemicals had been removed from the PEBBLEs. The PEBBLE solution was then passed through a suction filtration system (Fisher, Pittsburgh, PA) with a 2 μm Whatman anodisc filter to separate the larger size particles from the smaller ones. The filtrate (containing the smaller particles) was filtered again, this time with a 0.02 μm Whatman anodisc filter, to collect the particles which were then dried to yield a final product consisting of sol-gel PEBBLEs in the size range of 100–600 nm in diameter.[24]

2.3 *Imaging and optics*

Previous publications give the specific methods for calibration and imaging used for each specific matrix; acrylamide,[12–15] decyl methacrylate,[20] and sol-gel.[24]

Sensor calibrations were accomplished using either a FluoroMax-2 spectrofluorometer (ISA Jobin Yvon-Spex, Edison, NJ), slits set to 2 nm for both the emission and excitation, or an Olympus inverted fluorescence microscope, IMT-II (Lake Success, NY), using Nikon 50 mm f/1.8 camera lenses to project the image into an Acton 150 mm spectrograph (Acton, MA) with spectra read on a Princeton Instruments, liquid nitrogen-cooled, 1024 × 256 CCD array (Trenton, NJ), using a mercury arc lamp and an appropriate dichroic mirror module for wavelength selection.

Images of PEBBLE loaded cells were obtained using an Olympus FluoView 300 scanning confocal microscope system equipped with an Ar-Kr and He-Ne laser or an equivalent system. Data were acquired using the Olympus FluoView package.

2.4 *Cell culture*

Alveolar macrophages were recovered from rat lung lavage using Krebs-Henseleit buffer. Macrophages were maintained in a 5% CO_2, 37°C incubator in Dulbecco's Modified Eagle Medium (DMEM) containing 10% fetal bovine serum and 0.3% penicillin, streptomycin and neomycin. PEBBLE suspensions ranging from 0.3–1.0 mg/mL were prepared in DMEM and incubated with alveolar macrophage overnight.

Human neuroblastoma cells (cell line SH-SY5Y) were maintained in DMEM containing 10% fetal bovine serum and 0.3% penicillin, streptomycin and neomycin and subcultured into 60 mm petri dishes and incubated at 37°C in a 5% CO_2 environment. The cells were used when they reached a confluency of about 80%.

Rat C6-glioma cells were cultured in DMEM containing 400 mg/L D-glucose, 2 mM L-glutamine, 10% fetal bovine serum, 0.3% penicillin, streptomycin and neomycin and incubated at 37°C in a 5% CO_2 environment. Cells were released from culture dishes by trypsin treatment one day prior to the experiments and plated at a density of 150,000 cells per plate on uncoated 22 mm glass coverslips in 35 mm culture dishes.

3. Results and Discussion

3.1 *PEBBLE size distribution*

Each method for PEBBLE production has been optimized to produce uniform distributions of small particles, based on the specific matrix. A key requirement is the ability to collect these particles (dry) and then re-suspend them in aqueous solution. For acrylamide PEBBLEs, the described fabrication method gives a bi-modal distribution of 20-nm- and 200-nm-diameter particles.[12,13] The size of particles in this bi-modal distribution can be adjusted by changing the concentrations of the surfactants. These variously sized particles can be separated by filtration. Decyl methacrylate PEBBLEs range from 300–700 nm in diameter.[20] Sol-gel PEBBLEs are typically 100–600 nm in diameter.[24] Figure 1 shows SEM and TEM micrographs of acrylamide, decyl methacrylate, and sol-gel PEBBLEs. Recently all three have been made with dimensions below 100 nm in-house.

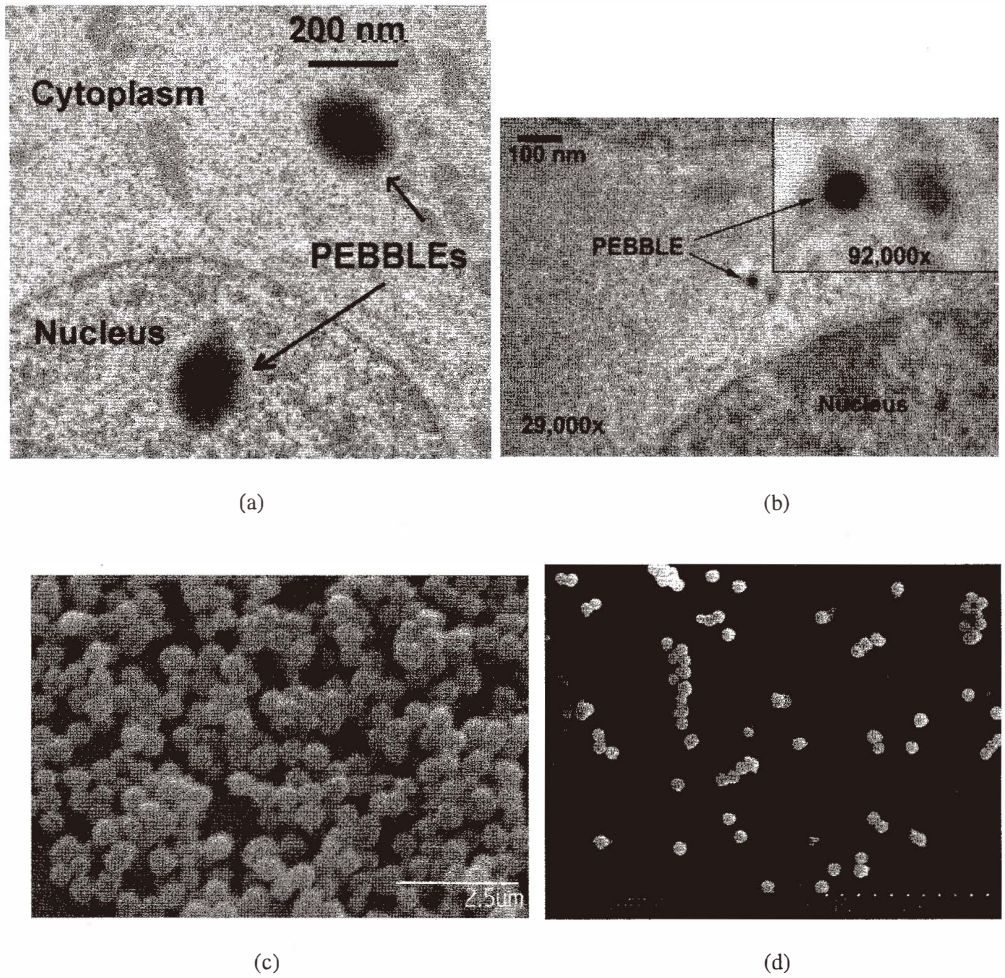

(a) (b)

(c) (d)

Fig. 1. (a–b) Transmission electron micrographs of PEBBLE sensors embedded biolistically (via gene gun), at 900 psi, into the cytoplasm of neuroblastoma cells: (a) Two 200 nm PEBBLEs, near or inside the cell nucleus. (b) One 20 nm PEBBLE next to a 1° lysosome in the cell cytoplasm. Original magnification is indicated in the figure and the inset. (c) SEM of gold coated decyl methacrylate PEBBLEs produced in emulsion polymerization with PEG 5´000 monoethyl ether as surfactant. Size distributions of 500 nm±40 nm =48% and 600 nm±40 nm =37% are found for the PEBBLEs produced. (d) Scanning electron micrograph showing the size distribution of sol-gel-PEG particles produced by the modified Stöber method (50% particles<200 nm).

3.2 *Polyacrylamide PEBBLE performance*

The major benefits of using a dye containing polyacrylamide matrix (compared to free dye alone) are the protection of the cell from dye cytotoxicity and of the dye from protein binding and other cellular processes, as well as the ability to include reference dyes in the sensing scheme. One example of the effect of protein binding is demonstrated with CNF pH dye. CNF is a highly photostable, ratiometric dye for pH, which is not used for intracellular applications because of the error induced by macromolecule binding. However, protected by the acrylamide matrix, CNF becomes a viable tool for intracellular pH study. Figure 2 illustrates the benefit of entrapping CNF in an acrylamide matrix. Incubation of the free dye with as little as 0.01% albumin induces alterations in emission ratios of almost 90% (pH was maintained constant as measured with a standard pH electrode) which is an error equivalent to 1 pH unit. The same dye, protected in the PEBBLE, shows minimal perturbation by albumin, with the resulting error equivalent to about one hundredth of a pH unit.

There is a wide range of available fluorescent dyes with good selectivity for pH and calcium. Thus calcium and pH sensing presented a good opportunity to compare PEBBLE response to that of a free dye in similar calibration environments. Complete details on these comparisons can be found in previously published work.[13,14] Tables 1 and 2 summarize the results for pH sensitive dyes and calcium dyes, respectively. Both dye solutions and PEBBLEs utilized the inert sulforhodamine 101 (SR) dye as an internal standard. It can be seen that, with few exceptions, in PEBBLEs the slope of the calibration decreases, resulting in reduced sensitivity of the measurements, but the linear ranges are not significantly affected by incorporating the dye in the PEBBLE. The acrylamide matrix does not adversely affect the reversibility of the indicator dye and can be tailored to entrap the dye for periods long enough to perform sensing in live cells. Figure 3 illustrates the reversibility of pH PEBBLEs containing the fluorescent pH probe CDMF and the reference

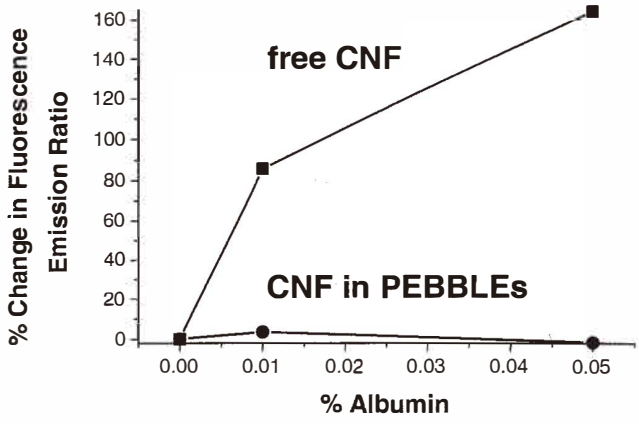

Fig. 2. Effect of protein on sensors.

Table 1
Results of calibrations of five pH sensitive dyes and the corresponding PEBBLE sensors. An internal standard, sulforhodamine 101, was added to each dye solution and was contained within the polymeric matrix of each PEBBLE sensor.
CNF: 5-(and 6-) carboxynaphthofluorescein
CDMF: 5-(and -6-) carboxy-4′,5′-dimethylfluorescein
BCPCF: 2′,7′-bis-(2-carboxypropyl)-5-(and-6)-carboxyfluorescein
FSA: fluorescein-5-(and -6)-sulfonic acid
SNAFL: 5-(and-6)-carboxy SNAFL®-1
SR: sulforhodamine 101

PH Indicator	Linear Range pH units	slope[a]±SD	intercept	r^2	n
CNF (dye)	7.0–7.7	7.8±0.4	–53	0.98	6
CDMF+SR (dye)	6.2–7.4	3.3±0.5	–19	0.96	12
BCPCF+SR (dye)	6.5–7.6	1.3±0.07	–7.3	0.99	6
FSA+SR (dye)	5.8–7.2	3.1±0.3	–17	0.99	7
SNAFL (dye)	7.2–7.7	–0.75±0.01	6.8	0.99	4
CNF (PEBBLEs)	7.0–7.7	0.24±0.01	–0.66	0.96	5
CDMF+SR(PEBBLEs)	6.2–7.4	0.67±0.05	–3.0	0.99	6
BCPCF+SR(PEBBLEs)	6.2–7.2	0.43±0.07	–1.6	0.90	6
FSA+SR (PEBBLEs)	5.8–7.0	3.4±0.4	–17	0.99	5
SNAFL (PEBBLEs)	7.2–8.0	–0.49±0.02	4.6	0.99	7

[a]Ratio of normalized fluorescence intensity vs pH.

Table 2
Results of calibrations of three calcium selective dyes and the corresponding PEBBLE sensors. An internal standard, sulforhodamine 101, was added to each dye solution and was contained within the polymeric matrix of each PEBBLE sensor.

Calcium Indicator	Linear Range μM calcium	slope±SD	intercept	r^2	n
Calcium Green+SR(dye)	0–0.15	30±0.7	1.7	0.94	4
Calcium Orange+SR(dye)	0–0.15	1.5±0.7	1.0	0.95	6
Calcium Green+ 5N SR(dye)	3–30	0.010±0.05	0.99	0.95	7
Calcium Green+SR(PEBBLEs)	0–0.15	7.3±0.05	0.97	0.99	6
Calcium Orange+SR(PEBBLEs)	0–0.1	1.3±0.05	1.0	0.79	5
Calcium Green+ 5N SR(PEBBLEs)	0–5	0.022±0.007	1.0	0.99	4

dye SR. The pH of the solution was varied between pH 6.4 and pH 7.0 for several cycles. The CDMF emission maximum was ratioed against the SR emission maximum and plotted, clearly demonstrating the full reversibility of the sensors. Assays of the leaching of CDMF, and calcium green PEBBLEs (each containing SR reference dye) show that less than 50% of each dye, leaches from the PEBBLEs in a 48 h time period. The leaching rates of all dyes were comparable. On the time scale of the current single cell experiments, usually a few hours, the dye loss is acceptable. With comparable leaching rates for

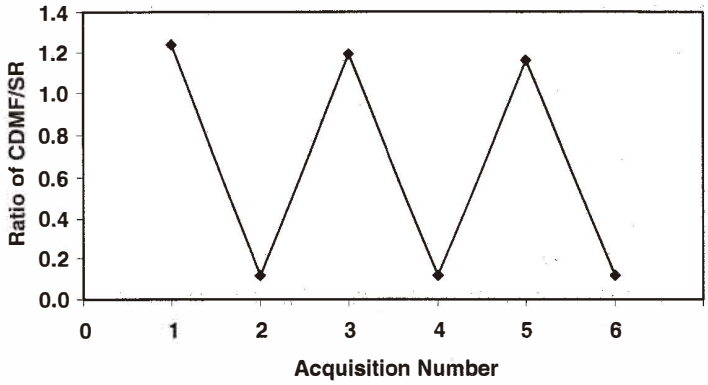

Fig. 3. The pH of a solution of CDMF/SR PEBBLEs was varied back and forth from pH 6.4 to pH 7.0, for several measurements. The ratio of the two peaks in the spectrum attained from each of the measurements was then plotted.

indicator and reference dyes, the problem is minimized due to the ratiometric sensing scheme used with these PEBBLEs.

3.3 *Decyl methacrylate (DMA) PEBBLE performance*

While the protection given by the acrylamide matrix prevents protein and macromolecule interference with sensing dyes, it does not prevent ion interference. In spite of advances in fluorescent indicator molecule development, there are still a good number of ions for which the most selective ionophores are nonfluorescent ("optically silent"). These ionophores stem from the century-long development of ion-selective electrodes (ISEs).

The fluorescence response scheme we used to follow analyte binding of nonfluorescent ionophores in DMA-based PEBBLE sensors closely follows much previous work on PVC -based fiber potassium-selective ion sensors.[10,25,26] The hydrogen-ion selective chromoionophore competes with the optically silent ionophore as cations enter the liquid polymer matrix. A lipophilic additive maintains ionic strength in the matrix and aids in preventing the co-extraction of anions. It allows for charge neutrality in the membrane without negative counter-ions being brought from the solution into the membrane.[10]

The work described here takes advantage of an indicator with two fluorescence emission maxima (λ_1,λ_2), giving a relative intensity that changes with the degree of protonation (Π). Π* can be evaluated in terms of the fluorescence intensity ratio, $F_{\lambda 2}/F_{\lambda 1}$, given by the protonated chromoionophore intensity $F_{\lambda 2}$ and the deprotonated chromoionophore intensity $F_{\lambda 1}$(see Fig. 4 for spectra).[25] The experimentally obtained spectra are normalized to the isoemmisive point of the dye and eq. (1) is used to determine the degree of protonation of the dye at any given analyte concentration at a known pH (superscripts P and D denote the completely protonated state and completely deprotonated state of the chromoionophore, respectively, lack of superscript denotes intermediate points)[20]:

* Π, the degree of protonation is equivalent to $(1-\alpha)$.[25]

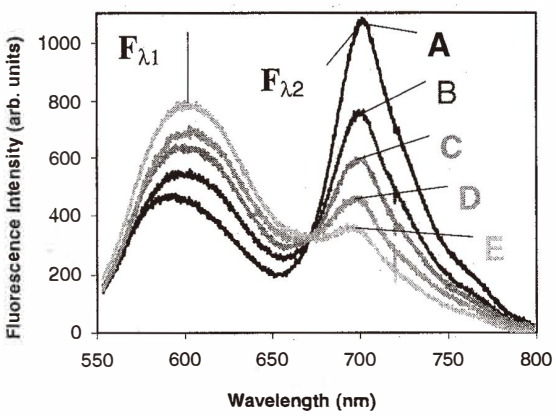

Fig. 4. Normalized emission spectra from suspended K^+ PEBBLE sensors using the pH chromoionophore ETH5350 for ion-correlation spectroscopy in tandem with BME-44 for the monitoring of K^+ activity. [A] 10 mM KCl, [B]50 mM KCl, [C] 200 mM KCl, [D] 500 mM KCl, and [E] 2.0 M KCl, all buffered at pH 7.2 with 10 mM Tris buffer.

$$\Pi = \frac{\dfrac{F^D_{\lambda 2}}{F^D_{\lambda 1}} - \dfrac{F_{\lambda 2}}{F_{\lambda 1}}}{\dfrac{F^D_{\lambda 2}}{F^D_{\lambda 1}} - \dfrac{F^P_{\lambda 2}}{F^D_{\lambda 1}} + \dfrac{F_{\lambda 2}}{F_{\lambda 1}}\left(\dfrac{F^P_{\lambda 2}}{F^D_{\lambda 1}} - 1\right)}. \tag{1}$$

The degree of protonation of the indicator spectra obtained from the PEBBLE calibration is related to the analyte concentration by using the theoretical treatment of ion-exchange sensors developed by Buhlmann *et al.*,[10] Bakker and Simon,[16] Morf *et al.*,[17] and Shortreed *et al.*[25] They defined Π as the relative portion of the protonated chromoionophore,[25] Π=[CH]/[C_{tot}]. Π is a function of the metal ion activity a_i^{v+} in solution, the hydrogen ion activity a_{H+} in solution, the interfering cations a_j^{z+} (where K^{opt}_{ij} is the selectivity coefficient for the interfering ion) and the constants [L_{tot}], [C_{tot}], [R_{tot}^-], which are total ionophore (ligand) concentration, total chromoionophore concentration, and total lipophilic charge site concentration, in the membrane. Note that [CH] is the protonated chromoionophore concentration and [C] is the free base concentration. The following equation has been shown to apply for a K^+ PEBBLE sensor when accounting for monovalent interfering cations.

$$a_i^v + K_{ij}^{opt} a_j^{z+} = \frac{1}{K_{exch}}\left(\Pi^{-1} - 1\right) a_{H+} \left(\frac{[L_{tot}]}{[R^-_{tot}] - \Pi[C_{tot}]} - 1 \right)^{-1} \tag{2}$$

Calibration of a K^+ sensor based on these principles is shown in Fig. 5. For potassium sensing the chromoionophore is ETH5350, the ionophore is BME-44, and the lipophilic additive is KTFPB.[20,26] The data points for potassium and sodium responses are plotted along with corresponding theoretical curves based on eq. (2). The constant K_{exch} is determined from a line fit to the experimental data. Then the theoretical curve is plotted using the experimentally determined K_{exch} and the constants R_{tot}, C_{tot} and L_{tot} to find the

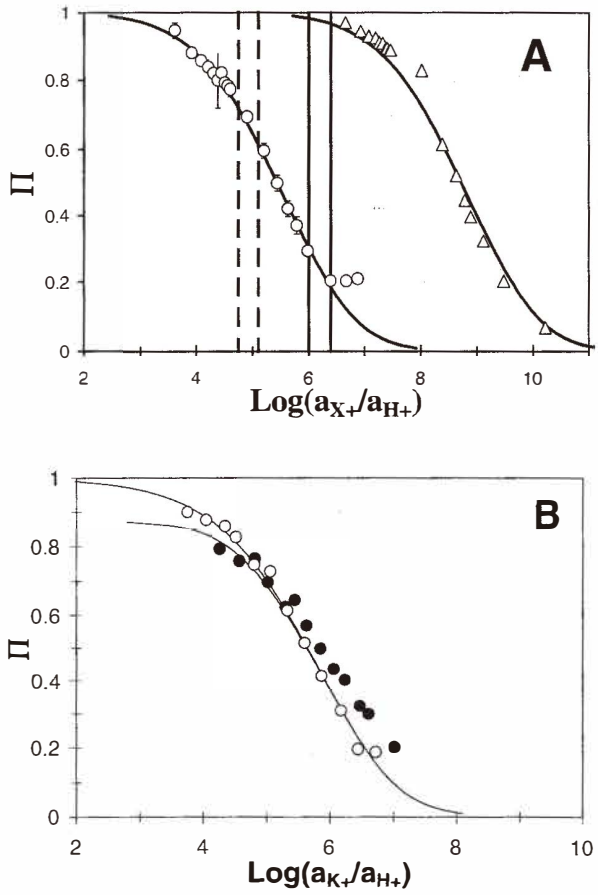

Fig. 5. (A) Response of BME-44-based decyl methacrylate PEBBLEs to potassium (○), and sodium (△), along with theoretical curves. Theoretical curves are constructed by solving eq. (2) for a_{Iv+}, (I+ being K^+ or Na^+ in this case), for a given value of P. The solid lines delimit values for log (a_{K+}/a_{H+}) typically found in intracellular media and the dashed lines delimit the typical extracellular ratios.[27] (B) Response of K^+ PEBBLEs to standard additions of KCl in tris buffer (○) compared to a similar experiment run in a constant background of 0.5 M Na^+ (●). The theoretical lines are drawn using eq. (2) with log $K^{opt}_{ij} = -3.3$.

expected a_{I+} for a given value of P. Dashed lines delimit typical extracellular activity ratios and the solid lines delimit the intracellular levels (log (a_{K+}/a_{H+})).[27]

We find that the response matches well with the theory, which is gratifying considering the small size of the systems. The dynamic range at pH 7.2 extends from 0.63 mM to 0.63 M a_{K+}. The log of the selectivity for potassium vs. sodium, determined by measuring the horizontal separation of the response curves at $\Pi = 0.5$, is –3.3. This value, when used to plot the expected response in a sample with a constant 0.5 M Na^+ interference, matches the experimental data obtained (see Fig. 5). This value indicates a selectivity similar to or better than that obtained for other and larger matrices incorporating BME-44, *e.g.*, –3.1 in PVC-based fiber optic work, and –3.0 in PVC-based microelectrodes.[26] It also exactly matches the value given in the review by Buhlmann *et al.*,[10] for a thin PVC film sensor. This selectivity should be more than sufficient for measurements in intracellular media where the potassium concentration[27] is about 100 mM and sodium is about 10 mM.

DMA based potassium sensors have a lifetime of 30 min due to component leaching from the liquid polymer membrane. This is consistent with the lifetime of PVC-based optodes of the same composition.[26] After 30 min the sensor response can deviate up to 7% from the initial calibration data at lower K^+ concentration. After 90 min the deviation is up to 13% at lower K^+ concentrations. The deviations are smaller at larger K^+ concentrations. However, as the PEBBLEs are single use sensors made for quick measurements inside cells that only survive for a short period of time, this is acceptable.

The sensors also prove to be fully reversible. Figure 6 shows the PEBBLEs, starting in an initial solution of 45 mM KCl which is diluted to 12 mM, then brought back to 45 mM by standard addition buffer and 2 M KCl solution.

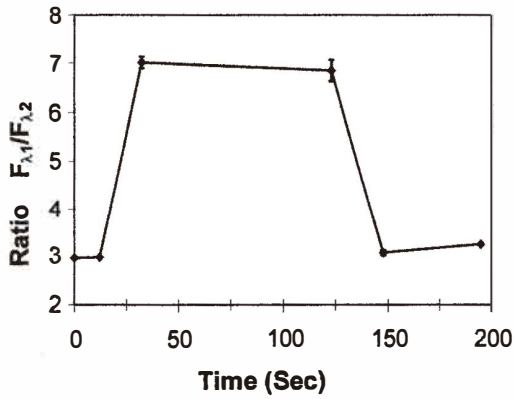

Fig. 6. Reversibility of K^+ sensitive PEBBLEs. The PEBBLEs started in 45 mM K^+, buffered at pH 7.2 with TRIS. The solution was then diluted with buffer to a concentration of 12 mM K^+; sufficient standard KCl solution was then added to bring the concentration of the solution back to 45 mM K^+.

3.4 *Sol-gel PEBBLE performance*

Oxygen is a key parameter in biological systems and is either produced by autotrophic photosynthesis in the presence of light, or consumed by different metabolic processes. For example, oxygen plays a crucial role in the cellular aerobic energy metabolism since it is used as an electron acceptor at the end of the aerobic pathway of glucose oxidation. Thus, knowledge of oxygen gradients in complex biological samples is of paramount importance for the understanding and quantification of these processes.[28,29] The numerous biological roles of molecular oxygen create the need for noninvasive, sensitive, and selective detection methods that are capable of real-time oxygen measurements.

The oxygen sensing sol-gel pebbles are based on the quenching of luminescence by oxygen. The oxygen quenching process is ideally described by the linear Stern-Volmer equation:

$$I_0/I = 1 + K_{SV}\, p[O_2],$$

where I_0 and I are the luminescence intensities in the absence and presence of oxygen at a partial pressure of $p[O_2]$, respectively, and K_{SV} is the Stern-Volmer constant, which depends directly upon the diffusion constant of oxygen, the solubility of oxygen, and the quenching efficiency and lifetime of the excited-state of the fluorophore.[30]

The fluorescence emission spectra of the sol-gel PEBBLE sensors, in different gaseous oxygen concentrations, are shown in Fig. 7. The sensor response was determined from the ratio (R) of the fluorescence intensities of $[Ru(dpp)_3]^{2+}$ to Oregon Green 488-dextran. These plots illustrate a number of features that are important to the optimization of the sensor design. The overall gas phase quenching response, Q_G, is given by:

$$Q_G = (I_{N2} - I_{O2}) / I_{N2}$$

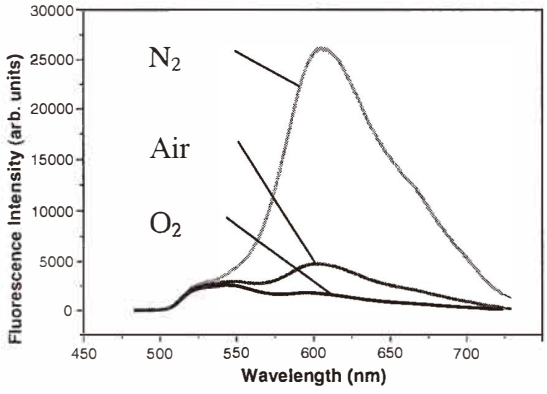

Fig. 7. Gaseous phase emission spectra of sol-gel oxygen PEBBLE sensors excited at 488 nm; top line: purged with N_2; middle line: in air; bottom line: purged with O_2. The peak on the left is the fluorescence emission of the reference dye (oregon green) and the peak on the right is the fluorescence emission of the indicator dye (ruthenium dye).

where I_{N2} and I_{O2} denote intensities in 100% N_2 and 100% O_2, respectively. The measured value of Q_G for the sol-gel PEBBLEs is ~92%. The calibration curve for the ratiometric sol-gel PEBBLEs showing the response to gaseous oxygen is displayed in Fig. 8. The quasi-linearity ($r^2 = 0.995$) of the Stern-Volmer plot implies a single fluorophore class accessible to molecular oxygen.[31] This data is in agreement with thin film sol-gel oxygen sensors[32] and has the advantage of being a ratiometric measurement.

The reversibility of the previously reported Ru-based sol-gel sensors in the gas phase has also been retained in these nanosensors.[24] Non-optimized measurements indicate that response times for a 90% oxygen concentration change should be well below 1 s, which is a direct result of the small size of the PEBBLEs. The sensors showed at least 98% recovery each time after the sensing environments were varied among air, oxygen and nitrogen saturated conditions.

Figure 9 shows the response of the TEOS based sol-gel PEBBLEs to dissolved oxygen (DO). The Q_{DO} for the sol-gel oxygen PEBBLEs is ~80%. (Quenching response to dissolved oxygen, Q_{DO}, is defined in a similar way to Q_G, where I_{N2} and I_{O2} are replaced by I in fully deoxygenated water and I in fully oxygenated water, respectively). This value represents a slight reduction in performance *vis-à-vis* gaseous oxygen; however, it is a great improvement with regards to TEOS-based sol-gel films.[33] These sol-gel films, made using TEOS as the precursor, had an excellent response to oxygen in the gas phase, i.e., Q_G = 90%, but a poor quenching response to dissolved oxygen, Q_{DO}, of only about 20%. MacCraith *et al.*[33] have subsequently reported significant improvements to the Q_{DO} ratio by preparing organically modified sol-gel (Ormosil) films using methyltriethoxysilane (MTEOS) and ethyltriethoxysilane (ETEOS) as the precursors. The success of the Ormosil films in raising the Q_{DO} ratio to 70–80% was largely attributed to the increased hydrophobicity of the film which reduced the water solubility in the film and caused the partitioning

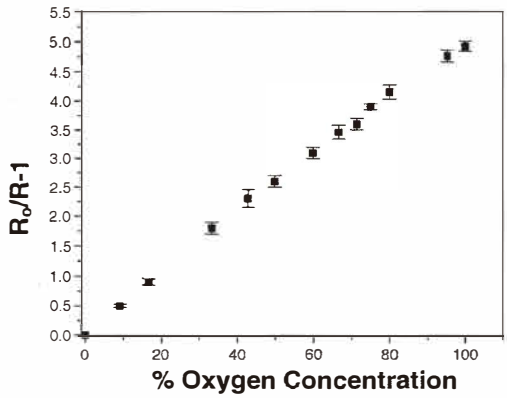

Fig. 8. Stern-Volmer plot of relative fluorescence intensity ratios for ratiometric sol-gel oxygen PEBBLEs in gaseous phase.

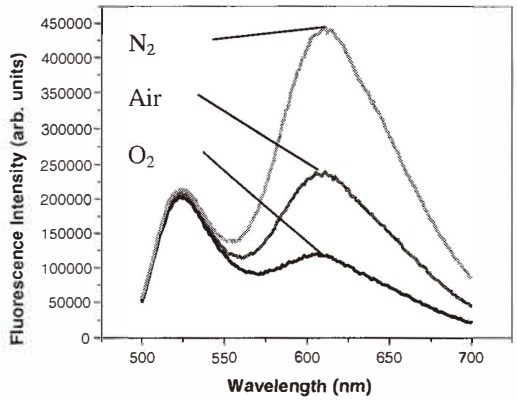

Fig. 9. Aqueous phase emission spectra of sol-gel oxygen PEBBLEs excited at 488 nm: top line: PEBBLE solution purged with N_2; middle line: PEBBLE solution purged with air; bottom line: PEBBLE solution purged with O_2.

of oxygen out of solution and into the film.[32] This would greatly increase the accessibility of oxygen molecules to the indicator dye molecules. It is thought that the high Q_{DO} response of the TEOS sol-gel PEBBLEs might be caused by the PEG content of the sensing matrix, PEG playing a role analogous to the Ormosil precursors and thus partitioning the oxygen preferentially into the sol-gel PEBBLEs. It is well known that oxygen has a higher solubility in organic liquids than in water,[34] so it should dissolve better in an organic phase compared to an aqueous phase. In summary, doping the sol-gel PEBBLEs with PEG adds organic components to the sensing matrix, thus encouraging the partitioning of oxygen into the matrix, and increases the accessibility of oxygen to the entrapped indicator dye molecules. This is in addition to the role of PEG in preventing particle aggregation in the PEBBLE sensor fabrication.

Figures 10 and 11 show the reversibility of the sol-gel PEBBLEs to changing dissolved oxygen concentrations and the Stern-Volmer plot of fluorescence intensity ratios to oxygen concentrations, respectively. This data shows that although the performance of the sol-gel PEBBLEs is slightly reduced in the aqueous phase, as opposed to the gas phase, the sensors still demonstrate good reversibility and reproducibility, as evidenced by the error bars in the calibration curve. The dashed line in Fig. 11 shows the extent of the biologically relevant regime of oxygen concentrations. We note that in this regime (from 0 to ~30 ppm oxygen), the Stern-Volmer plot is quasi-linear ($r^2 = 0.988$). The sensors showed at least 95% recovery each time the sensing environments were varied among air, O_2, and N_2 saturated sensor solutions.

Leaching of dye molecules out of the sol-gel matrix of the PEBBLE sensors is a major concern and is highly dependent on the dye. Factors such as the molecular size of the dye (small dyes can more readily diffuse through the pores and leak out of the matrix) and the solubility of the dye in the matrix and in water play a significant role.[24] Generally, sol-gel

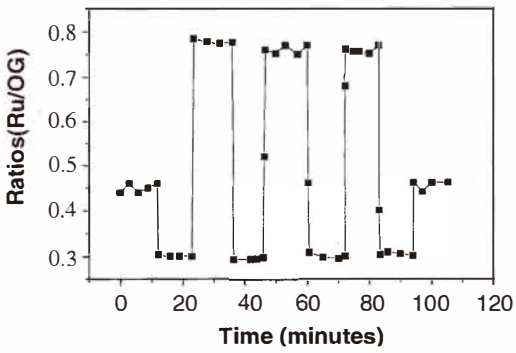

Fig. 10. Reversibility of PEBBLE sensor response to dissolved oxygen. Alternating measurements were taken in air-saturated, O_2-saturated and N_2-saturated PEBBLE sensor solutions.

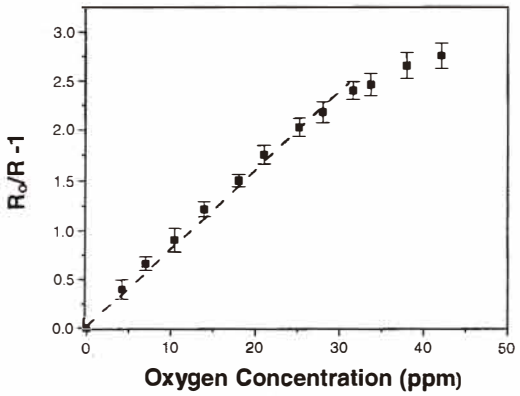

Fig. 11. Stern-Volmer plot of relative fluorescence intensity ratios for ratiometric sol-gel oxygen PEBBLEs in aqueous phase.

supports provide excellent stability with respect to dye leaching.[35] In particular, ruthenium complexes often have excellent stability inside the sol-gel matrix and in agreement with previous reports,[28,32,35–37] the indicator dye $[Ru(dpp)_3]^{2+}$ shows no signs of leaching. For the reference dye, the large size of the dextran molecular backbone to which the Oregon Green dye molecules are bound should greatly reduce leaching. Indeed, an investigation into the stability of the sol-gel PEBBLEs showed excellent stability of the sol-gel PEBBLE sensors with respect to dye leaching.[24] According to the dilution factor, a rough estimate provides an upper limit of 1% for the amount of dye molecules leached out of the sensing matrix over a three day period. In addition, we note again that the typical biological application is performed over a time scale of only a few hours.

We have found that the sol-gel matrix of PEBBLE sensors prevents macromolecules, such as proteins, from diffusing through the matrix (as expected). The matrix thus protects the entrapped dyes from the intracellular environment, preventing interference with the fluorescent properties of the dyes.[5] Without this shielding of a dye, its fluorescence would behave unpredictably inside a given cell, making calibration of even ratiometric dyes difficult or impossible. The effects of nonspecific protein binding were investigated by the addition of bovine-serum albumin (BSA, 5% solution), and the results are shown in Fig. 12 (a). Adding as little as 0.14% BSA to a solution containing $[Ru(dpp)_3]^{2+}$ and Oregon Green 488-dextran dye (at the same molar ratio in solution as inside the PEBBLEs) changed the fluorescence intensity ratio of the two dyes by a factor of more than 2.3 (i.e., an increase of

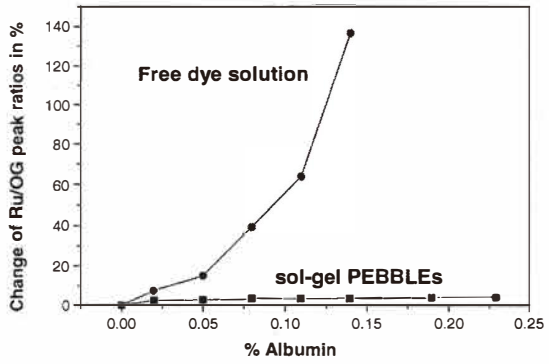

(a)

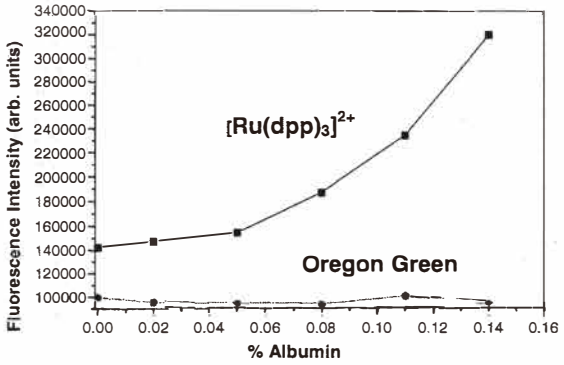

(b)

Fig. 12. (a) Effect of protein on sol-gel PEBBLEs and free dye solution. (b) Effect of protein on free dye molecules in solution. It is apparent that the fluorescence intensity of $[Ru(dpp)_3]^{2+}$ changed drastically upon interaction with BSA, while the intensity of Oregon Green remained largely unchanged.

over 130%). This change was mostly due to the change in the fluorescence intensity of $[Ru(dpp)_3]^{2+}$ after the addition of BSA, while the intensity of Oregon Green remained basically unchanged (Fig. 12(b)). However, under the same conditions, the PEBBLE sensors containing these two dyes were not affected by the addition of BSA and a change in fluorescence intensity ratio of at most 4% was observed even when an increased concentration of BSA (0.23%) was added, demonstrating the same protection as given to dyes in the acrylamide matrix.[13] The susceptibility of the sol-gel PEBBLEs to heavy metal ions (Hg^{2+} and Ag^{+}) and to one of the notorious collisional quenchers (I^{-}) was also examined.[24] $Hg(NO_3)_2$, $Ag(NO_3)$ and KI were added, respectively, to a PEBBLE solution and to a free dye solution of $[Ru(dpp)_3]^{2+}$ (same concentrations as in PEBBLEs) up to a concentration of about 200 ppm. There was a 5–10% decrease in the fluorescence intensity of the $[Ru(dpp)_3]^{2+}$ free dye each time, while for the PEBBLEs no measurable effect could be observed.

3.5 *Response time of PEBBLE nanosensors*

In order to follow biological perturbations in real time, a fast response is required from the PEBBLE sensors. Most PEBBLE sensors depend on bulk equilibrium between sensor and solution phase (the oxygen sensor depends on steady-state). The diffusion of analyte inside acrylamide and sol-gel should be similar to that in aqueous solution phase, while the diffusion of analyte in the hydrophobic DMA matrix is much slower. In all cases the small size of the PEBBLE sensors gives a rapid response time, despite the need for bulk equilibrium.

A reliable method for determining the response time of acrylamide sensors, to Ca^{2+}, used an Olympus IX50 inverted microscope equipped with a mercury arc lamp and a PMT. Calcium selective probes were premixed with a caged calcium ion, and this solution was inserted into a quartz capillary. The calcium was uncaged with a pulse of UV light from a Quanta-Ray 10 ns Nd/Yag laser (Quanta-Ray, Mountainview, CA) equipped with a frequency tripler and coupled into an optical fiber positioned over the capillary. In Fig. 13(a), the response time of the PEBBLE sensors was compared to that of the free dye (no polymer matrix), so as to separate the diffusion time through the solution from the diffusion time through the matrix. As can be seen, the 90% response time of the PEBBLE sensor to the increase in free calcium is on the order of *one millisecond or less*. Theoretically, with an approximate diffusion constant of 10^{-6} cm^2/s, the average diffusion time should be about ten microseconds for a 100-nm-radius sensor, and 100 nanoseconds for a 10-nm-radius sensor.

The measured transition times for sol-gel are on the order of 20–30 s, but these times are much longer than the intrinsic response time of the PEBBLEs, due to the significant contribution of the time used to saturate the solution with O_2 or N_2 (see Fig. 10). It is difficult to measure the exact response time, because changing between oxygenated and deoxygenated PEBBLE solutions itself takes time. The measured transition times (including the time of saturating the solution) are only an upper limit of the response time. We believe that the PEBBLE sensors should intrinsically have shorter response times than previously reported thin film and fiber optic sol-gel sensors (on the order of seconds or minutes) simply because of the smaller sizes of these sensors. According to the Einstein

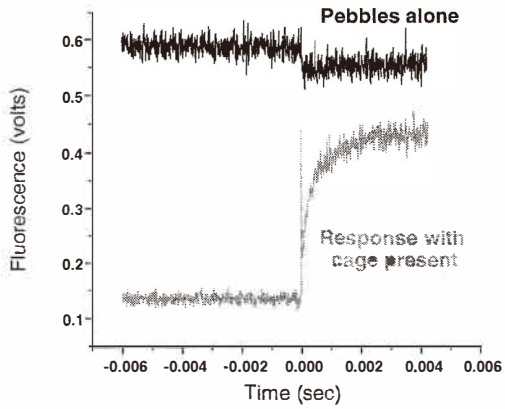

(a)

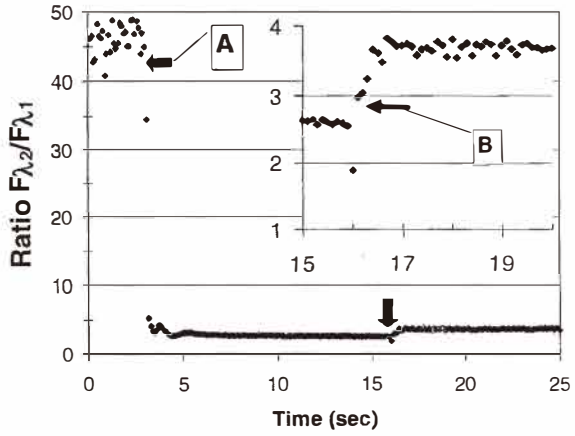

(b)

Fig. 13. (a) Response time of acrylamide PEBBLE sensors. Calcium was released using a single 10 ns UV pulse from a Nd/Yag laser which photolysed the cage, releasing free calcium into a solution of PEBBLEs. The observed response time, less than 1 ms, was indiscernible from that of the corresponding dye not entrapped in a polymer matrix. (b) Response time of K^+ sensitive PEBBLEs to added KCl and added buffer solutions. It can be seen that response in the forward direction is about 0.5 s (0–40 mM KCl, A) and the reverse (see inset) slightly longer (40–20 mM KCl, B), 0.8 s.

diffusion equation, where $X^2=2D\tau$, a shorter diffusion length X (which is directly related to the size of the sensor) results in a much shorter time for oxygen molecules to diffuse through the sensing matrix (which is basically the response time). A lower limit can thus be estimated, using $D\approx 2\times10^{-9}$ m^2/s (diffusion constant of oxygen in water) and $X\approx 3\times10^{-7}$ m,

giving $\tau \approx 20 \times 10^{-6}$ s, i.e. a response time in the microsecond range. An upper limit can be estimated considering that the PEBBLE sensor dimensions are 10–100 times smaller than those of thin film sensors, and have a spherical shape. This should give the PEBBLE sensors a response time in the millisecond range.

For DMA-based K^+ sensors, using BME-44 as the ionophore, ETH5350 as the chromoionophore and KTFPB as the ionic additive,[20] the ratio of the protonated chromoionophore to free base was analyzed vs. time in response time measurements. It was found (see Fig. 13(b)) that in going from log $a_{K+}/a_{H+} = 3.6$ to 5.7 the response time (10%–90% signal change) was about 0.5 s (for a concentration change of over 2 decades). In the reverse direction, the response was about 0.8 s. This fast, sub-second response time of the PEBBLEs is a direct result of their small size. Diffusion in decyl methacrylate is in the range of 10^{-8} cm^2/s, with small variations that depend on cross linker content.[38,39] Thus, for a PEBBLE radius of about 300 nm, we expect a diffusion time of about 10^{-3} s. This is consistent with the experimental values, which are again upper limit values due to the solution mixing times.

To summarize, using acrylamide or sol-gel PEBBLEs, one can monitor changes with response times on the microsecond timescale or, using the decyl methacrylate PEBBLEs, one can monitor changes on the 0.5 s time scale. Below are examples of some actual biological measurements taken with PEBBLE nanosensors.

3.6 *Biological applications of PEBBLE nanosensors*

An acrylamide PEBBLE selective for calcium (containing Calcium Crimson in the acrylamide matrix[40]) was produced in order to test for response to calcium flux in an intracellular environment. The PEBBLE sensors were also used to monitor calcium in phagosomes within rat alveolar macrophage, because of the ease with which macrophage phagocytosed the particles. This method for delivering the PEBBLEs into cells provided a simple, yet important, test of the PEBBLE sensors in a challenging (acidic) intracellular environment. Macrophage that had phagocytosed 20 nm calcium-selective PEBBLE sensors (Fig. 14) were challenged with a mitogen, Concanavalin A (Con A), inducing a slow increase in intracellular calcium, which was monitored over a period of 20 min (Fig. 14). PEBBLE clusters confined to the phagosome enabled the correlation of ionic fluxes with stimulation of this organelle.

Acrylamide PEBBLEs have also been utilized to observe the toxic effects of the industrial chemical DNB (*m*-dinitrobenzene).[14] Exposure to *m*-dinitrobenzene (DNB), a compound widely used as an industrial intermediate in the manufacture of dyes, plastics, and explosives, induces brain stem glio-vascular lesions in nuclei with high energy requirements, particularly those in the auditory pathway.[41] Neurotoxicity associated with DNB exposure is thought to be mediated by loss of ATP production secondary to the disruption of cellular redox potential.[42] Considering the potential of m-DNB to undergo redox cycling in the reducing environment of the mitochondrion, we have investigated whether disruption of mitochondrial function, subsequent to m-DNB exposure, resulted from an uncontrolled release of calcium associated with the onset of the mitochondrial permeability transition (MPT). Utilizing calcium selective PEBBLE sensors, it was discovered that the half-maximal rate of calcium release (EC_{50}) occurred at a 10-fold lower

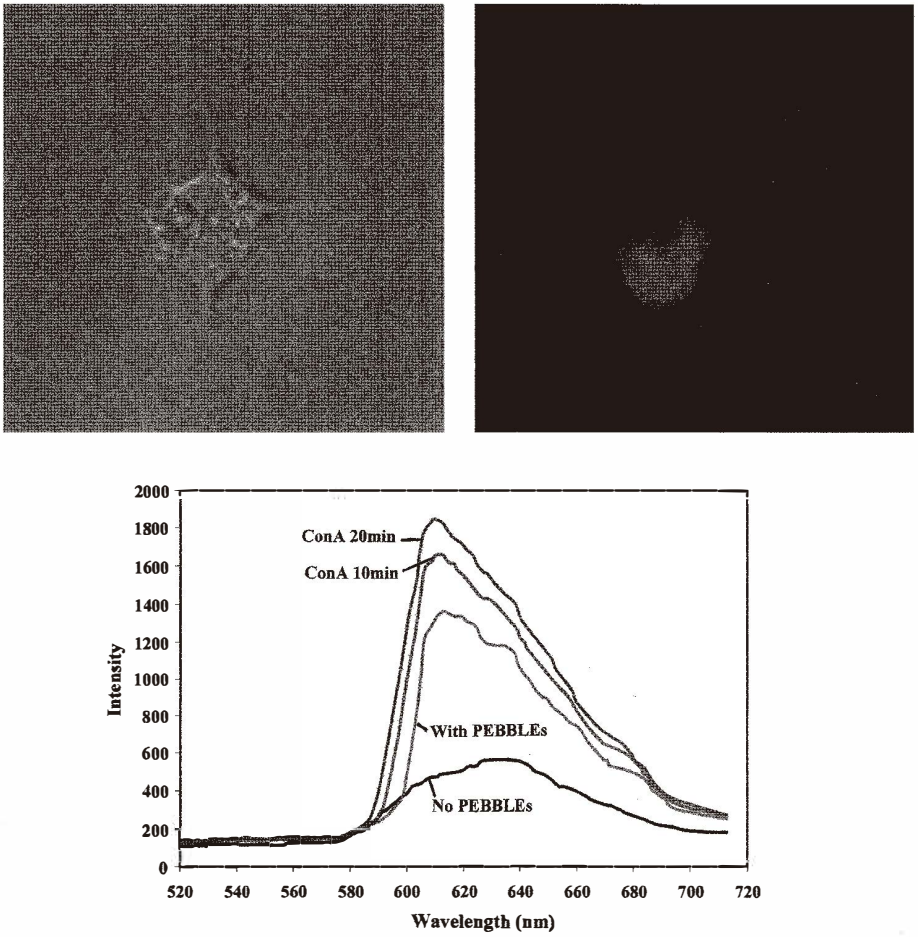

Fig. 14. *Top image.* Rat alveolar macrophage with calcium PEBBLE sensors (60×). *Left:* Nomarski illumination and *Right:* fluorescence illumination. *Bottom.* The increasing intracellular calcium, monitored by calcium PEBBLEs in alveolar macrophage following stimulation with 30 μg/mL Concanavalin A.

concentration of m-DNB in human SY5Y neuroblastoma cells than in human C6 glioma cells. This finding supports the hypothesis that sensitivity to m-DNB-induced calcium release is associated with differential regulation of the MPT in the cell lines evaluated. To further illustrate that the observed increases in cytosolic calcium are caused by release from intracellular stores, rather than disruption of the plasma membrane by m-DNB, cells containing calcium selective PEBBLE sensors were imaged using laser scanning confocal microscopy (Fig. 15). As in fluorimetry studies, increased cytosolic calcium was observed upon m-DNB exposure, as indicated by an increase in the fluorescence intensity of

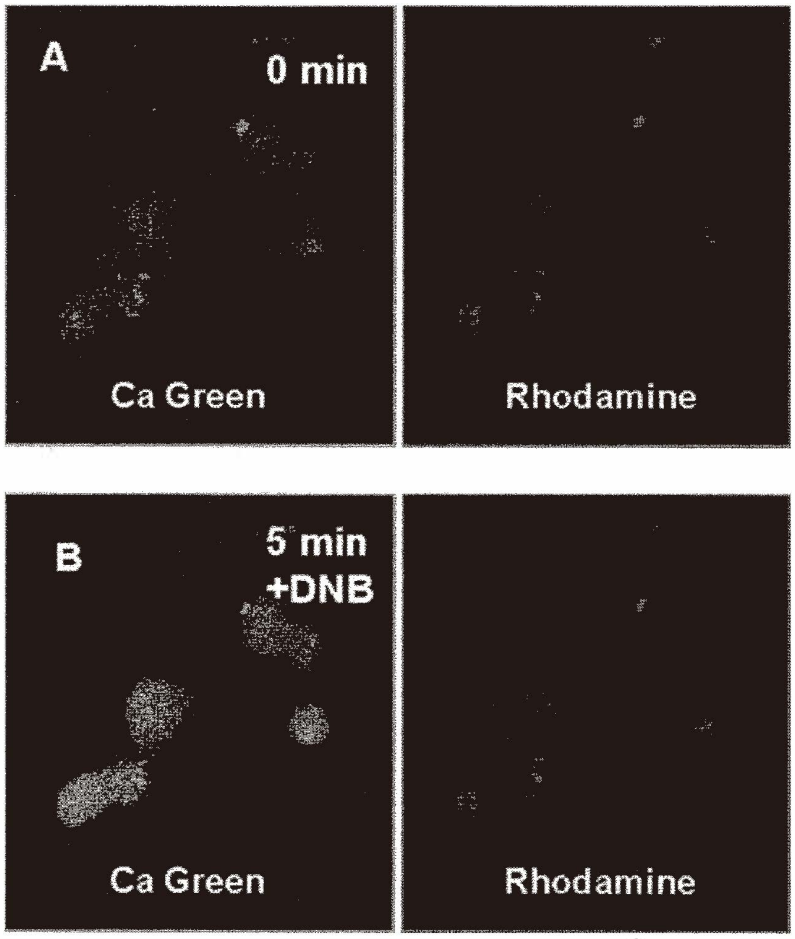

Fig. 15. Laser scanning confocal microscopy images of m-DNB-stimulated calcium release in SY5Y neuroblastoma cells lipofected with Calcium Green/SR PEBBLEs. Calcium Green and rhodamine fluorescence were monitored at time zero, prior to addition of m-DNB (A) and 5 min following addition (B).

Calcium Green-containing PEBBLE sensors.[14] The fluorescence intensity of the SR internal standard dye did not change following treatment with m-DNB, since it is inert with respect to ion concentration, thus demonstrating the utility of ratiometric PEBBLE sensors for measuring intracellular calcium fluxes.

In order to demonstrate how DMA PEBBLEs (400–600 nm) can be used for intracellular analysis, it is first necessary to introduce these sensors into the cells. The larger size of these liquid polymer PEBBLEs is prohibitive to liposomal delivery. Using the group's experience in introducing acrylamide PEBBLE sensors into cells[14,15] gene gun insertion

was chosen to insert the DMA PEBBLEs into cultured cells. DMA PEBBLEs were delivered into rat C6-glioma cells using a BioRad (Hercules, CA) Biolistic PDS-1000/He system at a firing pressure of 650 psi with a vacuum of 15 Torr on the system. A thin film of PEBBLEs suspended in water was dried on the target membrane. Following PEBBLE delivery, the cells were rinsed three times with Hanks 1× buffered salt solution and incubated in the same solution during analysis.[20]

Immediately following PEBBLE delivery, cells were placed on the INT-II Olympus inverted fluorescent microscope. The gating software for the CCD was set to take continuous spectra at 1.3 s intervals. After 20 s, and again after 60 s, 50 μL of 0.4 mg/mL kainic acid was injected into the microscope cell. Kainic acid is known to stimulate cells by causing the opening of ion channels. Confocal microscopy was used to determine the localization of the PEBBLE sensors after gene gun delivery. Figure 16(a) shows the confocal fluorescent image of the PEBBLEs overlaid with a Nomarski differential interference contrast image of the cells. The image indicates that the PEBBLE sensors are localized in the cytoplasm of the glioma cells. Figure 16(b) shows the PEBBLE sensors inside the cells responding to kainic acid addition to the cell medium, at 20 and 60 s. One can see that log (a_{K+}/a_{H+}) increases, indicating either an increase in K^+ concentration or a decrease in H^+ concentration (increase in pH). The amount of kainic acid added is not known to affect the pH of cells in culture. Thus the change is likely due to increasing intracellular concentration of K^+; this is the expected trend. The membrane of C6-glioma cells can initiate an inward rectifying K^+ current indicated by specific K^+ channels, a documented role in the control of extracellular potassium.[43] Thus when stimulated with a

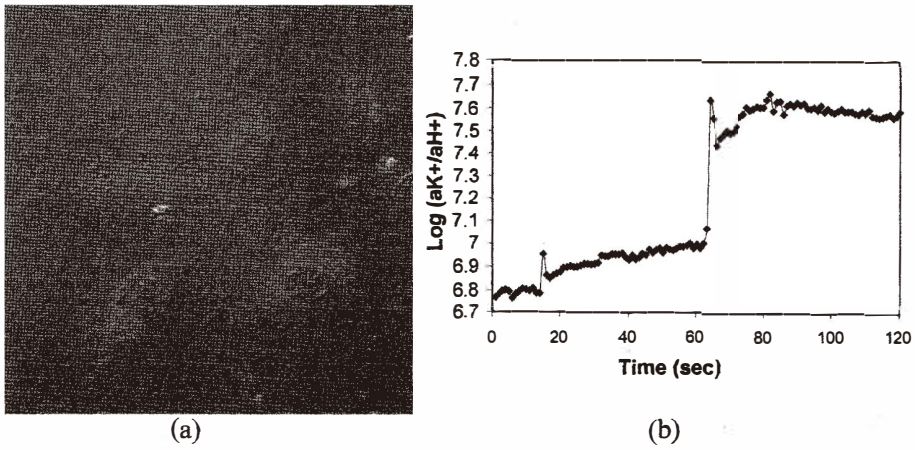

Fig. 16. (a) Confocal image of decyl methacrylate K^+ PEBBLE fluorescence, overlaid with Nomarski image of rat C6-glioma cells. 488 excitation, 580 long pass filter. (b) Ratio data of decyl methacrylate K^+ PEBBLEs in C6-glioma cells during the addition of kainic acid (50 μL of 0.4 mg/mL) at 20 s and at 60 s. Ratios were converted to log (a_{K+}/a_{H+}) using solution calibration of the PEBBLEs.

channel opening agonist, the K^+ concentration within the glioma cells is indeed expected to increase.

Sol-gel PEBBLEs were also delivered into rat C6-glioma cells using the BioRad gene gun system with the same parameters as described above. A thin film of PEBBLEs suspended in ethanol was dried on the target membrane. Following PEBBLE delivery the cells were rinsed with Dulbecco's phosphate-buffered saline (DPBS) and incubated with DPBS during measurements.[24]

Figure 17 (a) shows the confocal images of C6-glioma cells containing sol-gel PEBBLEs under Nomarski illumination. It can be seen that the cells still maintained their morphology after the gene gun injection of PEBBLEs and showed no indications of cell death. The fluorescence confocal images of these cells are presented in Fig. 17 (b) and 17 (c). The

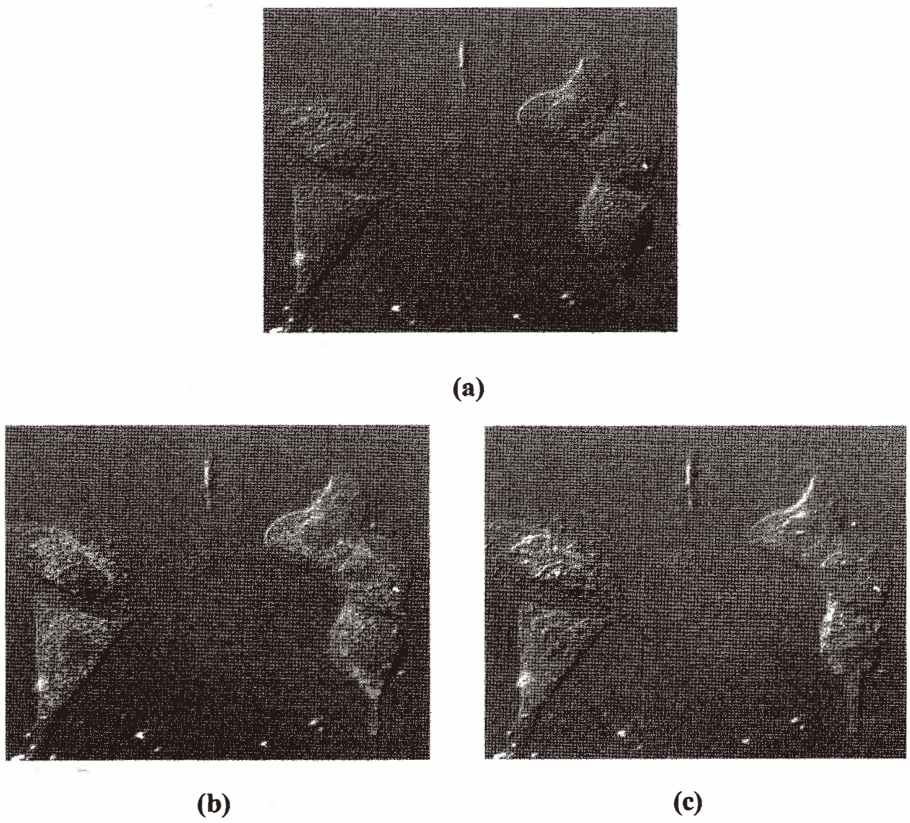

Fig. 17. Confocal images of rat C6-glioma cells loaded with sol-gel PEBBLEs by gene gun injection. (a) Nomarski illumination. (b) Oregon Green fluorescence of PEBBLEs inside cell overlaid with Nomarski illumination. (c) $[Ru(dpp)_3]^{2+}$ fluorescence of PEBBLEs inside cells overlaid with Nomarski illumination.

green fluorescence of Oregon Green 488-dextran and the red fluorescence of $[Ru(dpp)_3]^{2+}$ were excited, respectively, by reflecting the 488-nm (Ar-Kr) and 543-nm (He-Ne) laser lines onto the specimen, using a double dichroic mirror. The Oregon Green fluorescence from the PEBBLEs inside the cells (Fig. 17 (b)) was detected by passage through a 510 nm long-pass and a 530 nm short-pass filter, and the fluorescence of $[Ru(dpp)_3]^{2+}$ (Fig. 10 (c)) through a 605 nm (45 nm band-pass) barrier filter. A 40X, 1.4 NA oil immersion objective was used to image the Oregon Green and $[Ru(dpp)_3]^{2+}$ fluorescence. The distribution of PEBBLEs shown in the overlaid images (Fig. 17(b) and Fig. 17(c)) shows that the green and red fluorescence were truly from PEBBLEs inside cells. It should be noted that most of the PEBBLEs were loaded into the cytoplasm, but there were also some in the nucleus. Figure 18 shows the response of oxygen sensitive sol-gel PEBBLEs, inserted inside rat C6 glioma cells, to changing intracellular oxygen concentrations. After gene gun injection, the cells were immersed in DPBS and a spectrum was taken of these cells, using 480±10 nm excitation light. The air-saturated DPBS was then replaced by nitrogen-saturated DPBS, to cause a decrease in the intracellular oxygen concentration, and the response of the oxygen PEBBLE sensors inside the cells was monitored during a time period of 2 min. As can be seen, the fluorescence intensity of $[Ru(dpp)_3]^{2+}$ increased gradually as the oxygen level inside the cells decreased. Average intracellular oxygen concentrations were determined on the basis of the Stern-Volmer calibration curve, obtained using the fluorescence microscope-Acton spectrometer system, and are summarized in Table 3. The comparatively large errors are due to the low resolution of the spectrometer. We note that our measured intracellular oxygen value (when cells were in air-saturated DPBS) is comparable with the value of ~7.1 ppm measured inside the much larger islets of Langerhans.[44] These results show that the PEBBLE sensors are responsive when loaded into cells and that they retain their spectral characteristics, enabling a ratiometric measurement to be made.[24]

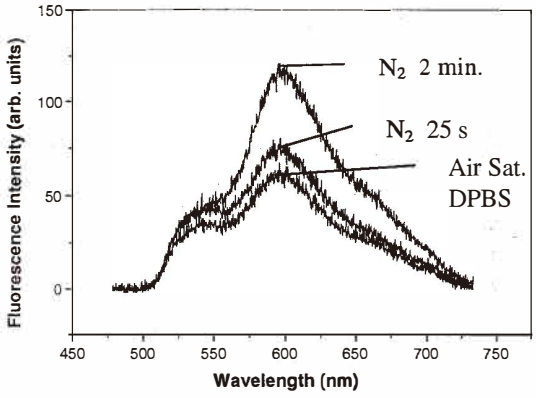

Fig. 18. Fluorescence spectra of a typical ratiometric sensor measurement of molecular oxygen inside rat C6-glioma cells; bottom line: cells (loaded with sol-gel PEBBLEs) in air-saturated DPBS; middle line: cells in N_2-saturated DPBS, 25 s after replacing the air-saturated DPBS; top line: cells in N_2-saturated DPBS, after 2 min.

Table 3
Real time measurements of intracellular oxygen.

	Average intracellular oxygen concentrations (ppm)
Cells in air-saturated buffer	7.9 ± 2.1
Cells in N_2-saturated buffer (after 25 s)	6.5 ± 1.7
Cells in N_2-saturated buffer (after 120 s)	≤ 1.5
Air-saturated buffer solution	8.8 ± 0.8

4. Concluding remarks

We have established polyacrylamide, polydecyl methacrylate and silica sol-gel hybrids as viable platforms for the construction of nanooptical fluorescent probes (PEBBLEs). The use of established microemulsion protocols for acrylamide and the addition of PEG stabilization for decyl methacrylate and sol-gel particles has allowed us to reach submicron diameter sizes. A PEBBLE with a 20 nm radius only occupies 1 ppb of a standard mammalian cell (assumes 20 μm radius). This allows for insertion of a host of PEBBLEs into a single viable cell, with little mechanical or chemical perturbation of the cellular environment. All three classes of PEBBLE preserve the basic bio-compatibility principle: No interference between cell and PEBBLE. This is achieved by encapsulating the indicator dye inside the matrix, in contrast to other strategies, where the active groups are on the outer surface of the nanoparticle.

The three matrices allow one to use a variety of sensing schemes so as to tailor PEBBLEs for the specific monitoring of any analyte for which selective probes are available. Fluorescent free dyes, optically silent ionophores, proteins, and enzymes are all viable options for the construction of PEBBLEs by choosing the correct matrix platform. So far PEBBLEs have been developed for H^+, Ca^{2+}, K^+, Na^+,Mg^{2+}, Zn^{2+}, Cl^-,NO_2^-, O_2, NO, and glucose. The utility of ratiometric measurements, along with the tandem use of dyes in order to create ratiometric sensors, has been demonstrated. Also demonstrated was the ability to use highly selective but nonfluorescent ("optically silent") ionophores in nanooptical PEBBLEs. The theory describing ion exchange in micron-sized polymer films also works for nanometer sized decyl methacrylate PEBBLEs. The flexibility in the composition of the matrix and sensor components permits this design to be used for a number of different analytes and analyte concentrations. The small size allows for novel intracellular studies.

Initial studies have also shown that the new PEBBLEs can be delivered to viable cells and these cells can be observed in a time resolved manner, responding to changes in their environment. The small size of the PEBBLE sensors allows for the insertion of more than one type of sensor. The second sensor could be spectrally resolved from the primary sensors in either emission or excitation, or the PEBBLE concentration could be adjusted so that signals from single PEBBLEs can be resolved spatially. In this manner one could study complex biological responses, where a host of changes may occur in response to a single agonist; this could be done in a single viable cell, and in real time. PEBBLEs are an excellent tool for gaining further understanding of biological processes.

Acknowledgment

The authors thank Steve Parus for instrumentation expertise, Susan Barker for technical assistance, Professor Mark E. Meyerhoff and Theresa M. Ambrose for help in the initial stages of utilizing DMA and Maria J. Moreno for assistance with the data normalization formalism for DMA PEBBLEs, Rhonda Lightle and Chris Edwards for transmission electron microscopy, the University of Michigan Transgenic Core for technical assistance, and the University of Michigan Electron Microbeam Analysis Laboratory (funded in part by NSF grant EAR-9628196) for use of the SEM. We also gratefully acknowledge NIH Grants 2R01-GM50300-04A1 (Kopelman) and R01-ES08846 (Philbert) for funding, as well as NCI Contract N01-CO-07013.

Reference

1 J. Slavik: Fluorescent Probes in Cellular and Molecular Biology (CRC Press: Boca Raton, FL, 1994).
2 W. T. Mason: Biological Techniques (Academic Press: San Diego, CA, 1993).
3 R. Nuccitelli: Methods in Cell Biology (Academic Press: San Diego, CA, 1994).
4 B. Herman: Fluorescence Microscopy, 2 ed. (Springer: New York, NY, 1998).
5 M. L. Graber, D. C. DiLillo, B. L. Friedman and E. Pastoriza-Munoz: Analytical Biochemistry **156** (1986) 202.
6 M. CohenKashi, M. Deutsch, R. Tirosh, H. Rachmani and A. Weinreb: Spectrochimica Acta Part A-Molecular and Biomolecular Spectroscopy **53** (1997) 1655.
7 C. C. Overly, K. D. Lee, E. Berthiaume and P. J. Hollenbeck: Proceedings of the National Academy of Sciences of the United States of America **92** (1995) 3156.
8 B. Morelle, J. M. Salmon, J. Vigo and P. Viallet: Cell Biology and Toxicology **10** (1994) 339.
9 W. N. Ross: Biophysical Journal **64** (1993) 1655.
10 P. Buhlmann, E. Pretsch and E. Bakker: Chemical Reviews **98** (1998) 1593.
11 W. Tan, R. Kopelman, S. L. R. Barker and M. T. Miller: Analytical Chemistry **71** (1999) 606A.
12 H. A. Clark, S. L. R. Barker, R. Kopelman, M. Hoyer and M. A. Philbert: Sensors and Actuators B **51** (1998) 12.
13 H. A. Clark, M. Hoyer, M. A. Philbert and R. Kopelman: Analytical Chemistry **71** (1999) 4831.
14 H. A. Clark, R. Kopelman, R. Tjalkens and M. A. Philbert: Analytical Chemistry **71** (1999) 4837.
15 H. A. Clark, M. Hoyer, S. Parus, M. Philbert and R. Kopelman: Mikrochimica Acta **131** (1999) 121.
16 E. Bakker and W. Simon: Analytical Chemistry **64** (1992) 1805.
17 W. E. Morf, K. Seiler, B. Lehmann, C. Behringer, K. Hartman and W. Simon: Pure & Applied Chemistry **61** (1989) 1613.
18 K. Kurihara, M. Ohtsu, T. Yoshida, T. Abe, H. Hisamoto and K. Suzuki: Analytical Chemistry **71** (1999) 3558.
19 K. Suzuki, H. Ohzora, K. Tohda, K. Miyazaki, K. Watanabe, H. Inoue and T. Shirai: Analytica Chimica Acta **237** (1990) 155.
20 M. Brasuel, R. Kopelman, T. J. Miller, R. Tjalkens and M. A. Philbert: Analytical Chemistry **73** (2001) 2221.
21 I. Tsagkatakis, S. Peper and E. Bakker: Analytical Chemistry **73** (2001) 315.
22 S. Peper, I. Tsagkatakis and E. Bakker: Analytica Chimica Acta **442** (2001) 25.

23 D. R. Uhlmann, G. Teowee and J. Boulton: Journal of Sol-Gel Science and Technology **8** (1997) 1083.
24 H. Xu, J. W. Aylott, R. Kopelman, T. J. Miller and M. A. Philbert: Analytical Chemistry **73** (2001) 4124.
25 M. Shortreed, E. Bakker and R. Kopelman: Analytical Chemistry **68** (1996) 2656.
26 M. R. Shortreed, S. Dourado and R. Kopelman: Sensors and Actuators B **38–39** (1997) 8.
27 D. Ammann: Ion-Selective Microelectrodes (Springer: Berlin, 1986).
28 I. Klimant, F. Ruchruh, G. Liebsch, A. Stangelmayer and O. S. Wolfbeis: Mikrochimika Acta **131** (1999) 35.
29 I. Lahdesmaki, L. D. Scampavia, C. Beeson and J. Ruzicka: Analytical Chemistry **71** (1999) 5248.
30 J. N. Demas and B. A. DeGraff: Analytical Chemistry **63** (1991) 829A.
31 W. Xu, R. Scmidt, M. Whaley, J. N. Demas, B. A. DeGraff, E. K. Karikari and B. A. Famer: Analytical Chemistry **67** (1995) 3172.
32 C. M. McDonagh, B.D. MacCraith and A.K. McEvoy: Analytical Chemistry **70** (1998) 45.
33 A. K. McEvoy, C. M. McDonagh and B. D. MacCraith: Analyst **121** (1996) 785.
34 The Merck Index 12th edition; Merck&Co: NJ, 1996.
35 C. M. Ingersoll and F. V. Bright: Chemtech **27** (1997) 26.
36 M. L. Bossi, M. E. Daraio and P. F. Aramendia: Journal of Photochemistry Photobiology A **120** (1999) 15.
37 M. T. Murtagh, M. R. Shahriari and M. Krihak: Chemical Materials **10** (1998) 3862.
38 T. M. Ambrose and M. E. Meyerhoff: Electroanalysis **8** (1996) 1095.
39 T. M. Ambrose and M. E. Meyerhoff: Analytical Chemistry **69** (1997) 4092.
40 H. A. Clark, Ph.D Dissertation, Ph.D Thesis,University of Michigan, Ann Arbor, 1999.
41 J. L. Holton, C. C. Nolan, S. A. Burr, D. E. Ray and J. B. Cavanagh: Acta Neuropathologica **93** (1997) 159.
42 M. A. Philbert, C. C. Nolan, J. E. Cremer, D. Tucker and A. W. Brown: Neuropathology & Applied Neurobiology **13** (1987) 371.
43 A. Emmi, H. J. Wenzel and P. A. Schwartzkroin: Journal of Neuroscience **20** (2000) 3915.
44 S. -K. Jung, W. Gorski, C. A. Aspinwall and L. M. Kauri: Analytical Chemistry **71** (1999) 3642.

About the Authors

Dr. Raoul Kopelman and Dr. Martin A. Philbert have a continuing collaboration for the development, characterization, and application of nanodevices for sensing, imaging, and therapeutic applications on the subcellular level. PEBBLEs, the sensing element of these endeavors, are serving as the developmental platform for both imaging and therapeutic applications.

Dr. Raoul Kopelman is the Kasimir Fajans Collegiate Professor of Chemistry, Physics and Applied Physics. A member of the Biophysics Program, he is also formally associated with the University of Michigan Centers for Ultrafast Optics and for Biologic Nanotechnology. Dr. Kopelman is an expert in laser chemistry, optical materials science and nanofabrication of optochemical sensors and actuators. He is also an expert on spectroscopy, molecular excitonics, reaction kinetics in confined domains, and Monte Carlo simulations on phase transitions and surface chemistry. Dr. Kopelman received his Ph.D. from Columbia University in 1960 and served as a postdoc in chemical physics at

Harvard, 1960–62, and after that as Senior Research Fellow at Caltech. He has served as a Professor of Chemistry at the University of Michigan since 1966. In 1991 he was made a Professor of Chemistry & Physics and a member of the Biophysics Program at the University of Michigan. In 1994 he was made The Kasimir Fajans Collegiate Professor of Chemistry, Physics & Applied Physics at the University of Michigan. In 1998 he was a founding member of the University of Michigan Biologic Nanotechnology Center at the Medical School. Dr. Kopelman's broad range of research interests in analytical and physical chemistry has led to more than 400 peer-reviewed publications.

Dr. Martin A. Philbert is a Professor of Toxicology and is a neurotoxicologist and experimental neuropathologist with expertise in the biochemical and pathologic outcomes of exposure to toxic chemicals. In 1988 Dr. Philbert received his Ph.D. in neurochemistry/ biochemistry from the London Univ., Royal Postgrad. Medical School and served as a postdoc. in neurotoxicology at Rutgers University from 1988–1990. From 1990–1995 he served as a research Assistant Professor in Neurotoxicology at Rutgers University and has been a member of the Michigan Toxicology faculty since 1995. The expertise of Dr. Martin A. Philbert is essential to the study of PEBBLE sensor delivery, function, and effectiveness as applied to living biological systems.

Graduate students and postdoc researchers who play and have played a key role in PEBBLE development in Dr. Kopelman's lab include the following:
Dr. Murphy Brasuel (Ph.D., 2002) played a role in liquid polymer PEBBLE production (decyl methacrylate PEBBLEs for K^+, Na^+, and Cl^-), (1996-present).
Dr. Jonathan W. Aylott (postdoc 1998–2001) worked on sol-gel and acrylamide PEBBLE development (oxygen and glucose sensing). He is currently a Lecturer of Analytical Chemistry at the University of Hull, UK.
Dr. Heather Clark (Ph.D., 1999) was a key player in initial PEBBLE studies, including work on O_2, Ca^{2+}, H^+, and Mg^{2+} acrylamide PEBBLEs as well as initial studies on liquid polymer PEBBLE development as well cell delivery method exploration. She is currently a Postdoctoral Fellow at the Center for Biomedical Imaging Technology and Department of Physiology, University of Connecticut Health Center.
Hao Xu played a role in sol-gel and acrylamide PEBBLE development for oxygen and glucose sensing (1996–present).

Graduate students and postdoc researchers who play and have played a key role in PEBBLE biological application in Dr. Philbert's lab include:
Dr. Marion Hoyer (postdoc 1997–1999) assisted in the initial stages of PEBBLE delivery to cells and in designing biologically relevant experiments for PEBBLE application. She is currently working on automobile regulations for air quality with the EPA.
Terry J. Miller (1997–present) is currently involved in culturing of cells and running the confocal microscope experiments involving PEBBLEs in single cells.
Dr. Ron Tjalkens (postdoc 1999–2001) was instrumental in setting up confocal experiments for PEBBLE application in the study of DNB toxicity. He is currently an Assistant Professor of Toxicology and Neuroscience in the Department of Interdisciplinary Toxicology at Texas A&M University.